



Pressure-induced structural phase transition and electrical properties of Cu₂S

Xue Yang^a, Shu-Qing Jiang^a, Hui-Chao Zhang^a, Kun-Peng Zhao^b, Xun Shi^b, Xiao-Jia Chen^{a, c, *}

HPSTAR
654-2018



^a Key Laboratory of Materials Physics, Institute of Solid State Physics, Chinese Academy of Sciences, Hefei 230031, China

^b State Key Laboratory of High Performance Ceramics and Superfine Microstructure, Chinese Academy of Sciences, Shanghai 200050, China

^c Center for High Pressure Science and Technology Advanced Research, Shanghai 201203, China

ARTICLE INFO

Article history:

Received 11 February 2018

Received in revised form

21 June 2018

Accepted 3 July 2018

Available online 5 July 2018

Keywords:

Copper sulfides

Structural phase transition

In situ electrical measurement

Diamond anvil cell

High-pressure

ABSTRACT

The structural phase transition and electrical properties of Cu₂S have been investigated by X-ray diffraction and electrical resistance measurements at pressures up to 41.3 GPa in diamond anvil cell. A new high pressure phase is found above 22.3 GPa, which probably has a tetragonal structure. It is observed that the electrical resistance exhibits an insulating behavior at high pressures and low temperature. After the pressure is released, the high pressure phase transforms back to original monoclinic phase. This study sheds light on the electrical transport properties of Cu₂S, as well as to improve our understanding of its high pressure phase transition behavior.

© 2018 Elsevier B.V. All rights reserved.

1. Introduction

Over the past few decades, copper sulfides have attracted much attention due to the rich phases, complex structures and excellently tunable properties [1–10]. Cu_{2-x}S (0 < x ≤ 1) has been known for an important P-type semiconductor [4], and it has been extensively investigated for its structural complexity and potential applications in battery solar cells [5], electrodes [6], switching [7], photocatalysis [10], sensing devices [11], superionic materials [12], etc. Extensive efforts have been carried out to investigate the structural behavior and properties of Cu_{2-x}S.

Cu₂S provides an intriguing and representative example for investigating various questions in condensed matter physics [13], which is helpful to the understanding of the functional and quantum materials. It is a fast ionic conductor [14] with highly mobile Cu ions. Especially, Cu₂S has the high thermoelectric performance and the maximum *zT* value of 1.7 at 1000 K [8]. Stoichiometric Cu₂S exhibits a monoclinic phase with space group *P21/c* [15]. It is of great interest to study the structural phase transitions of Cu₂S

[16–19]. Recently, it has attracted considerable interest due to structural fluctuations in Cu₂S [20,21]. Tao et al. [22] reported that the concurrent pumping and probing of Cu₂S nanoplates using an electron beam can directly manipulate the transition, and this new structure manipulation method is in a controlled and reversible fashion.

High-pressure is a powerful tuning parameter that has been used to modify the crystal structure and tune the band structures and properties of materials [23–28]. To our knowledge, there are only two high pressure studies on Cu₂S, and it is found that Cu₂S undergoes a series of phase transitions under high-pressure. Wang et al. [29] found that Cu₂S nanowires undergo two high pressure phase transitions (original monoclinic phase–high pressure monoclinic phase–hexagonal phase) at 2.4 GPa and 4.4 GPa, respectively. Recently, Santamaria-Perez et al. [30] carried out high-pressure X-ray diffraction measurements on bulk Cu₂S up to 30 GPa, two different high-pressure monoclinic phases were found at 3.2 and 7.4 GPa, respectively. Above 26 GPa, a third pressure-induced transition occurs in Cu₂S. However, the crystal structure of this new high pressure phase remains unknown. On the other hand, the structure of Cu₂S is unclear when the pressure is released to ambient conditions. It is an interesting and fundamental scientific question to find out whether the new high pressure phase can be

* Corresponding author. Key Laboratory of Materials Physics, Institute of Solid State Physics, Chinese Academy of Sciences, Hefei 230031, China.

E-mail address: xjchen@issp.ac.cn (X.-J. Chen).

preserved in Cu_2S .

Motivated by the novel phase transition and unique properties change by the application of high-pressure, how the properties of Cu_2S can be tuned by pressure is also an interesting question. However, there is no research on the electrical properties of copper sulfides at high pressures. In addition, exploring the electrical properties of Cu_2S is a matter of interest in band-gap engineering and functional materials designing. Therefore, we focus on the pressure effect on electrical behavior of Cu_2S .

Herein, we present the results of the structural phase transition and electrical transport properties on Cu_2S studied by the combination of synchrotron X-ray diffraction and *in-situ* high-pressure electrical resistance measurement in the diamond anvil cell. A new pressure-induced phase transition on Cu_2S is found above 22.8 GPa. And the electrical properties of Cu_2S under high-pressure are explored.

2. Experimental details

The Cu_2S samples were prepared by directly melting the elements Cu and S in sealed silica tubes under vacuum. Details of the synthesis are given elsewhere [8]. High-pressure experiments were carried out by using a diamond anvil cell (DAC) with a culet size of 300 μm . The T301 stainless steel gasket was preindented to 50 μm , and then a center hole of 100 μm diameter was drilled as the sample chamber. This chamber was filled with a small amount of samples and a tiny ruby chip. Silicon oil was loaded together with samples as a pressure transmitting medium in high-pressure X-ray diffraction (XRD) experiments. The *in situ* high-pressure XRD experiments were carried out up to 41.3 GPa using angle dispersive X-ray diffraction (ADXRD) ($\lambda = 0.6199 \text{ \AA}$) at the Beijing Synchrotron Radiation Facility (BSRF). The sample-to-detector distance and the image plate orientation angles were calibrated using CeO_2 standards. All of our XRD patterns were integrated to give one-dimensional powder diffraction patterns using the FIT2D program [31], yielding one-dimensional intensity versus diffraction angle 2θ patterns. High pressure electrical resistance measurements were performed by using quasi-four-probe method in a DAC with anvils of 300 μm culet. The platinum foil was used as electrode probe, and a thin BN layer acted as an electric insulator between the electrodes leads and the metal gasket. The samples were placed in the chamber without any pressure transmitting medium. Pressure was gauged by means of ruby fluorescence method in our experiments [32].

3. Results and discussion

At ambient conditions, Cu_2S crystallizes in monoclinic phase with a space group $P2_1/c$ [13]. In the monoclinic form, the sulfur lattice frame is a distorted hexagonal, whereas the copper atoms partially occupy the lattice sites and are organized in a complex fashion, forming a 144-atoms unit cell [13], the crystal structure is shown in Fig. 1.

The pressure evolution of the angle-dispersive powder X-ray diffraction data of Cu_2S is shown in Fig. 2. A typical XRD pattern of Cu_2S collected at 1.0 GPa is indexed to the monoclinic phase (JCPDF Card no. 23596) with a space group $P2_1/c$. With increasing pressure, all the diffraction peaks shift to larger angles, indicating a pressure-induced reduction of d-spacing or shrinkage of the lattice parameters. Upon compression, there are several changes in the XRD patterns. At around 3.8 GPa, it can clearly be seen that the shape and intensity of the peaks are distinct from low pressure patterns. As shown in Fig. 2, some peaks disappear and several new peaks appear, indicating that a phase transition from original monoclinic phase (phase I) to phase II occurs at 3.8 GPa. Upon further

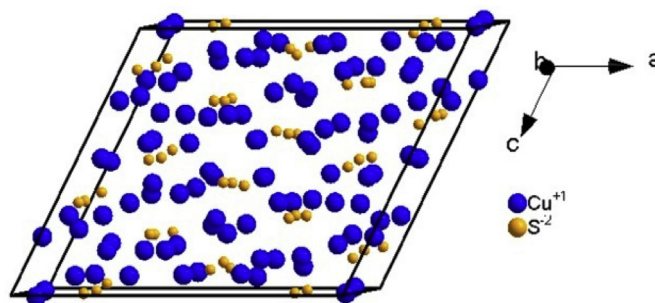


Fig. 1. Crystal structure of Cu_2S at ambient conditions. Blue and yellow circles represent Cu and S atoms, respectively. (For interpretation of the references to colour in this figure legend, the reader is referred to the Web version of this article.)

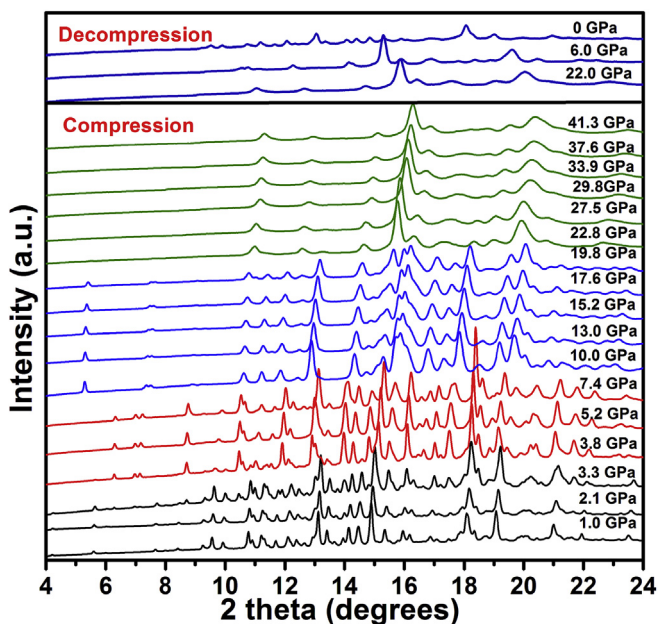


Fig. 2. Synchrotron X-ray diffraction patterns of Cu_2S during the compression from ambient conditions to 41.3 GPa ($\lambda = 0.6199 \text{ \AA}$) and decompression.

compression, there are several obvious changes in the XRD patterns in the number, intensity and shape of the peaks, suggesting that a phase transition takes place at 10.0 GPa (phase III). When the pressure increased to 22.8 GPa, obvious changes in the diffraction are observed at this pressure. Some peaks of phase III disappear, the changes suggest that Cu_2S undergoes a phase transition (phase IV). The diffraction peaks of the new high pressure phase (phase IV) can be stable up to the highest pressure of 41.3 GPa that we have performed. Upon decompression, the high pressure phase IV of Cu_2S can persist down to 6.0 GPa. This is in good agreement with the previous result [30]. There is no XRD data were collected below 5.3 GPa in their experiment, so when the pressure is back to ambient pressure, how the structure change is not clear. In our study, when the pressure is released to ambient conditions, Cu_2S transforms back to the initial monoclinic structure (as shown on the top of Fig. 2).

The Pawley refinement of Cu_2S was used to obtain the structural parameters. The background, zero shift, and lattice parameters were refined. Fig. 3 shows the refinement of XRD pattern of Cu_2S at 19.8 GPa with the $R_{wp} = 2.8\%$ and $R_p = 2.2\%$, respectively. The fitting results show that the diffraction patterns of phase II and phase III could be clearly indexed using the different monoclinic structures

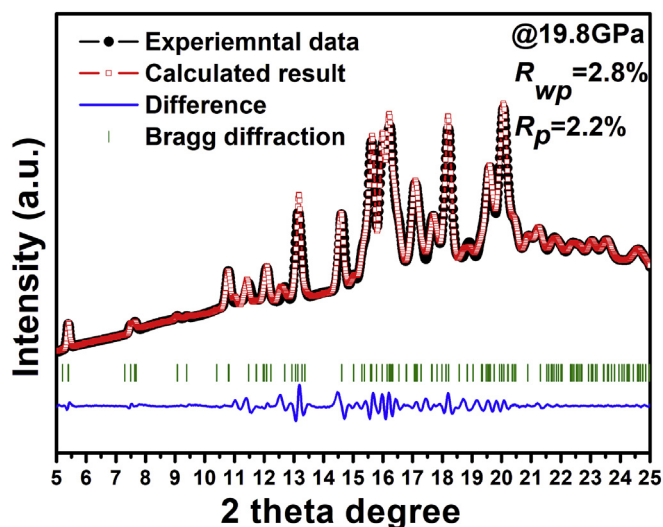


Fig. 3. The Pawley refinement of the diffraction pattern of Cu_2S at 19.8 GPa. Black, red and blue symbols represent experimental, calculated, and differences, respectively. Green bars are marked at the positions of diffraction peaks. (For interpretation of the references to colour in this figure legend, the reader is referred to the Web version of this article.)

which were reported in previous results [30]. The structural parameters are shown in Table 1. The high pressure phase II and III are both the monoclinic structure but with the different space group [30]. The phase transition behavior of Cu_2S below ~ 20 GPa is in agreement with previous report [30], but it is different from Cu_2S nanomaterial [29]. Above ~ 20 GPa, Cu_2S undergoes a new phase transition to phase IV in this study. However, influence of non hydrostaticity [33,34], the diffraction peaks become broad and weak with the increasing pressure. We attempted to determine the structure of phase IV, and found that the X-ray diffraction of phase IV can be indexed to tetragonal phase. We also tried to deduce the fine structure of this phase but it is not successful due to the overlapping and broad diffraction peaks.

The lattice parameters of Cu_2S upon compression as a function of pressure are depicted in Fig. 4. The lattice parameters a , b and c are decreased with the increasing pressures. At 3.8 GPa and 10.0 GPa, the lattice parameters were changed accompanying the structural phase transitions. The variation of relative lattice parameters is shown in Fig. 4. The normalized lattice parameters indicate that Cu_2S shows an anisotropic compressibility. The pressure dependence of the unit cell volume is shown in Fig. 5. It can be clearly seen that the unit-cell volume decreases with pressures in both the low and high pressure regions. By fitting the third-order Birch-Murnaghan equation of state [35],

$$P = \frac{3K_0}{2} \left[\left(\frac{V}{V_0} \right)^{\frac{2}{3}} - \left(\frac{V}{V_0} \right)^{\frac{5}{3}} \right] \left\{ 1 + \frac{3}{4} (K'_0 - 4) \left[\left(\frac{V}{V_0} \right)^{\frac{2}{3}} - 1 \right] \right\}$$

where K_0 is the isothermal bulk modulus, V_0 is the volume per formula unit at ambient pressure, and V is the volume per formula unit at pressure P given in GPa. A fit to the P - V curve yields a bulk

modulus $K_0 = 44$ (5) GPa and its pressure derivative $K'_0 = 4$ for the original low-pressure monoclinic phase, and the ambient pressure volume $V_0 = 46.6$ (0.3) \AA^3 . The fit to the P - V data yields the bulk modulus $K_0 = 553.1$ (8) GPa, 89 (8) GPa, the pressure derivatives $K'_0 = 3, 6$, and the volume $V_0 = 45.8$ (0.6) $\text{\AA}^3, 42.9$ (0.4) \AA^3 for the high pressure phase II and phase III, respectively.

The fitting results show that the diffraction patterns of phase II and phase III could be clearly indexed using the different monoclinic structures which were reported in previous results [30]. The structural parameters are shown in Table 1. The high pressure phase II and III are both the monoclinic structure but with the different space group [30]. The phase transition behavior of Cu_2S below ~ 20 GPa is in agreement with previous report [30], but it is different from Cu_2S nanomaterial [29]. Above ~ 20 GPa, Cu_2S undergoes a new phase transition to phase IV in our study. We attempted to determine the structure of phase IV, and found that the X-ray diffraction of phase IV can be indexed to tetragonal phase. We also tried to deduce the fine structure of this phase but it is not successful due to the overlapping and broad diffraction peaks. The compression behavior of Cu_2S is similar as the previous result [30]. It is important to note that the value of K_0 obtained from original monoclinic phase ($P21/c$) is smaller than the obtained K_0 in high pressure phases, suggesting the harder bonds at high-pressure phases. Our results clearly show that, as expected, Cu_2S become more incompressible with increasing pressure, but the variation of K_0 is not so pronounced. The percentage of volume decrease during the phase transitions are about 2.5% and 4.1%, respectively. This is in good agreement with the previous reports [29,30].

Fig. 6 displays the electrical resistance of Cu_2S at various pressures and room temperature. During compression, several discontinuities are observed from the electrical resistance at ~ 4.1 GPa, ~ 7.8 GPa and ~ 18.8 GPa. Especially, when the pressure exceeds 18.8 GPa, resistivity shows a clear increasing trend with increasing pressure. These changes suggest that the structural phase transitions take place in Cu_2S . Upon decompression, the resistance is decreased from 50 GPa to 6.9 GPa. Below 6.9 GPa, the resistance become to increase, which may be inferred that the high pressure phase IV persist to 6.9 GPa, and then it transforms to the original monoclinic phase. Both the XRD results and electrical properties provide consistent evidence for the pressure-induced phase transitions.

The electrical resistance of Cu_2S at high pressures and low temperature are plotted in Fig. 7. At ambient pressure, the resistance of Cu_2S increases with the low temperature down to about 4 K. The result indicates that Cu_2S exhibits an insulating behavior with the decreasing temperature. Upon compression, the low-temperature resistance of Cu_2S is increased. It is observed that Cu_2S still shows the insulating behavior at low temperature until the highest pressure ~ 41.9 GPa in this study. Compared to Cu_2Se , the resistance behavior of Cu_2S shows the obviously different behavior [36]. Chi et al. found that a possible charge density wave (CDW) transition occurs in Cu_2Se at ambient pressure and low temperature [36,37]. The origin of this different electrical transport behavior is not clear. Further theoretical and experimental efforts are needed to explore the properties and transformation mechanisms.

Table 1
Unit cell for the three different monoclinic phases of Cu_2S .

Phase	Crystal	a (\AA)	b (\AA)	c (\AA)	β ($^\circ$)	Pressure (GPa)
Phase I	monoclinic	15.2450	11.8224	13.3965	116.4188	1.6 GPa
Phase II	monoclinic	10.3702	6.7947	7.4428	100.45	3.8 GPa
Phase III	monoclinic	6.940	6.685	6.702	93.2	10.0 GPa

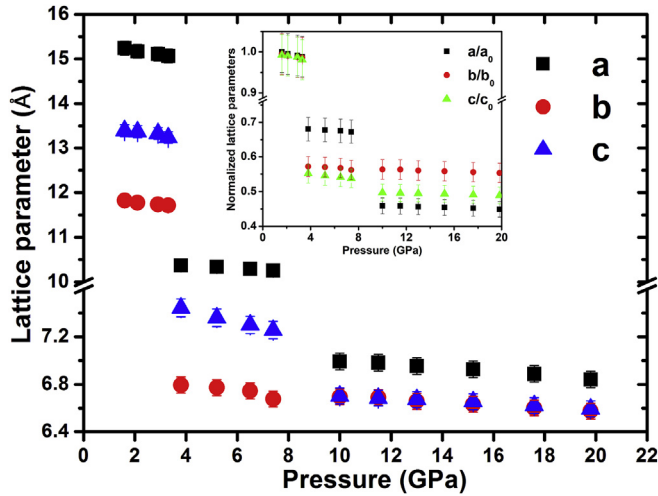


Fig. 4. Lattice parameters of Cu_2S under high pressure. Inset: Variation of relative lattice parameters a/a_0 , b/b_0 and c/c_0 for Cu_2S .

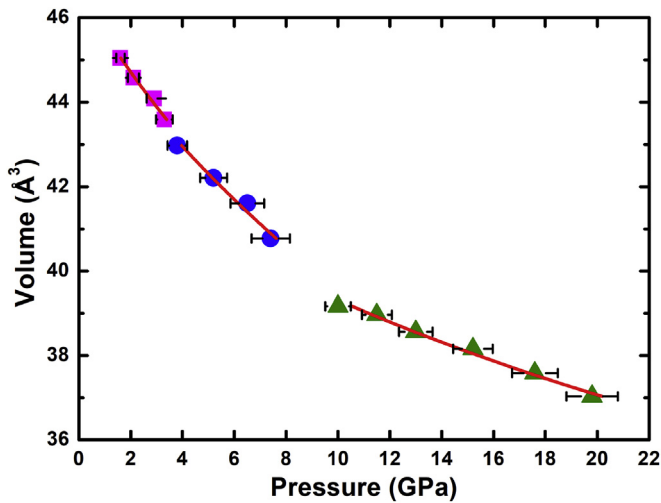


Fig. 5. Plot of pressure-volume data of Cu_2S .

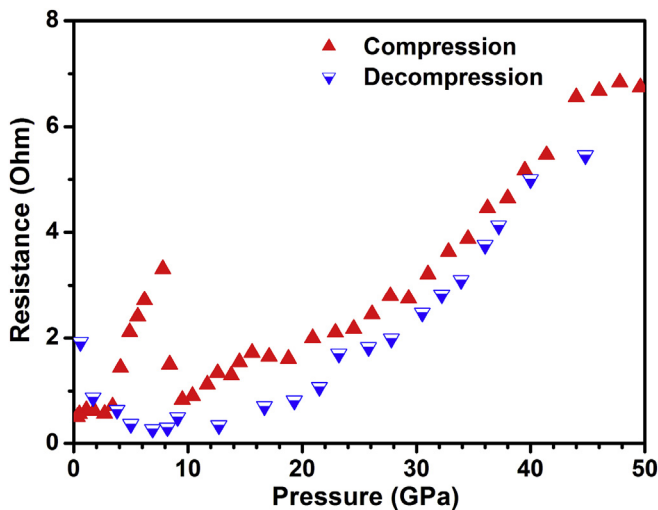


Fig. 6. Pressure dependence electrical resistance of Cu_2S during compression and decompression at room temperature.

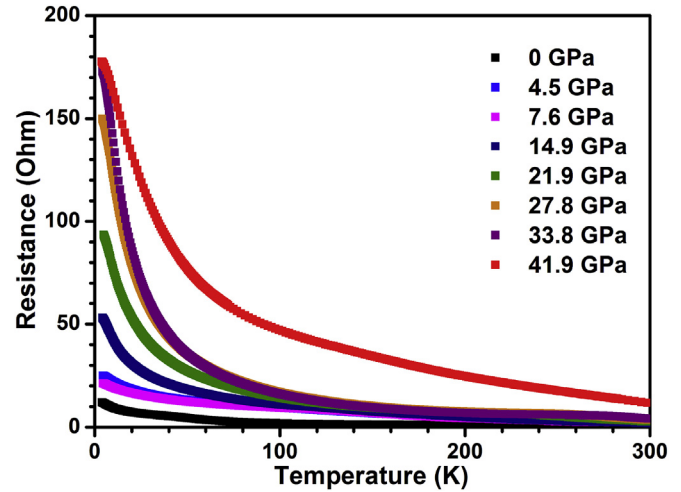


Fig. 7. Temperature dependence of the electrical resistance of Cu_2S at selected pressures.

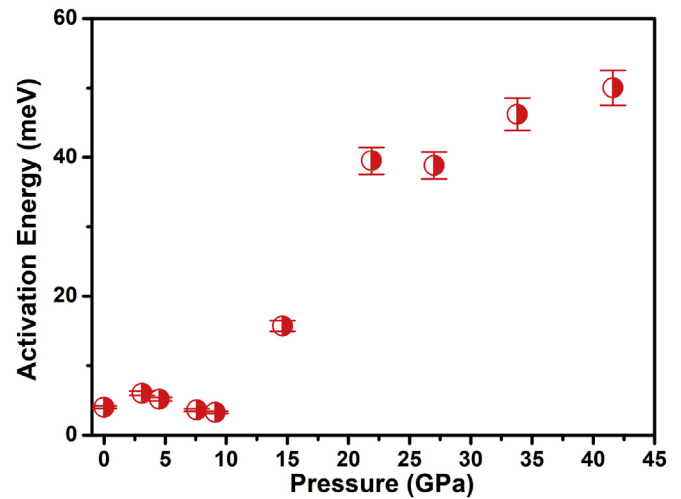


Fig. 8. Pressure dependence of the activation energy of Cu_2S .

To understand the deeper insight into the electrical transport behavior of Cu_2S under compression, the carrier transport activation energy can be deduced from the temperature-dependent resistance curve. It was found that the $\ln R$ vs. $1/T$ curves of Cu_2S match well with the Arrhenius forum. Hence, we can estimate E_t in the 50–100 K range from Arrhenius equation [38]:

$$\ln R \propto \frac{E_t}{2k_B T}$$

where R is the resistance, k_B is Boltzmann's constant, E_t is the activation energy of the carrier, and T is the temperature. From Fig. 8, it can be clearly seen that there are three kinks at 3.5 GPa, 9.1 GPa and 21.9 GPa, which are influenced by the structural phase transitions. It is generally known the pressure effect on the energy barriers to the charge transport can be expressed by the change of E_t vs pressure. In addition, the positive slope above 21.9 GPa suggests that the carrier transport becomes harder and the carrier concentration decreases with increasing pressure.

4. Conclusions

In summary, we have investigated the structural phase transition and electrical transport properties of Cu₂S by combined synchrotron X-ray diffraction and the electrical resistance measurement. It is found that two structural phase transitions occur at 3.8 GPa and 10.0 GPa from the monoclinic *P21/c* phase to high pressure monoclinic phases. Upon further compression, a new phase transition takes place at 22.8 GPa, it is proposed that the high pressure phase maybe has a tetragonal structure. The electrical resistance results indicate that Cu₂S represents the insulating behavior at high pressures and low temperature.

Acknowledgments

This work was supported by National Natural Science Foundation of China (grant No. 11604342, No. 11504382, No. 51727806), Science Challenge Project of China (No. TZ2016001) and was partly sponsored by Program of Shanghai Subject Chief Scientist (16XD1403900). The authors are grateful to Xiaodong Li, Yanchun Li and Pengshan Li for their help during the synchrotron radiation experimental research and Jianbo Zhang for his help in the high pressure electrical measurements.

References

- [1] H.T. Evans, *Am. Mineral.* 66 (1981) 807.
- [2] R. Blachnik, A. Müller, *Thermochim. Acta* 361 (2000) 31.
- [3] X. Sun, H.T. Deng, W.G. Zhu, Z. Yu, C.Z. Wu, Y. Xie, *Angew. Chem. Int. Ed.* 55 (2016) 1704.
- [4] Y.X. Zhao, H.C. Pan, Y.B. Lou, X.F. Qiu, J.J. Zhu, C. Burda, *J. Am. Chem. Soc.* 131 (2009) 4253.
- [5] W.S. Chen, J.M. Stewart, R.A. Mickelsen, *Appl. Phys. Lett.* 46 (1985) 1095.
- [6] J.S. Chung, H.J. Sohn, *J. Power Sources* 108 (2002) 226.
- [7] P.H. Liu, C.C. Lin, A. Manekathodi, L.J. Chen, *Nano Energy* 15 (2015) 362.
- [8] Y. He, T. Day, T.S. Zhang, H.L. Liu, X. Shi, L.D. Chen, G.J. Snyder, *Adv. Mater.* 26 (2014) 3974.
- [9] H. Lee, S.W. Yoon, E.J. Kim, J. Park, *Nano Lett.* 7 (2007) 778.
- [10] A. Manzi, T. Simon, C. Sonnleitner, M. Döbblinger, R. Wyrwich, O. Stern, J.K. Stolarczyk, J. Feldmann, *J. Am. Chem. Soc.* 137 (2015) 14007.
- [11] A.A. Sagade, R. Sharma, *Sens. Actuators B* 133 (2008) 135.
- [12] J.L. Wang, K.M. Chen, M. Gong, B. Xu, Q. Yang, *Nano Lett.* 13 (2013) 3996.
- [13] R.M. Fernandes, A.V. Chubukov, J. Schmalian, *Nat. Phys.* 10 (2014) 97.
- [14] R.J. Cava, F. Reidinger, B.J. Wuensch, *Solid State Ionics* 5 (1981) 501.
- [15] H.T. Evans, *Nat. Phys. Sci.* 232 (1971) 69.
- [16] D.J. Chakrabarti, D.E. Laughlin, *Bull. Alloy Phase Diagrams* 4 (1983) 254.
- [17] Q. Xu, B. Huang, Y.F. Zhao, Y.F. Yan, R. Noufi, S.-H. Wei, *Appl. Phys. Lett.* 100 (2012), 061906.
- [18] K. Okamoto, S. Kawai, *Jpn. J. Appl. Phys.* 12 (1973) 1130.
- [19] M.J. Buerger, B.J. Wuensch, *Science* 141 (1963) 276.
- [20] H.M. Zheng, J.B. Rivest, T.A. Miller, B. Sadtler, A. Lindenberg, M.F. Toney, L.W. Wang, C. Kisielowski, A.P. Alivisatos, *Science* 333 (2011) 206.
- [21] L.W. Wang, *Phys. Rev. Lett.* 108 (2012), 085703.
- [22] J. Tao, J.Y. Chen, J. Lia, L. Mathurinb, J.-C. Zheng, Y. Lie, D.Y. Lu, Y. Cao, L.J. Wu, R.J. Cavag, Y.M. Zhu, *Proc. Natl. Acad. Sci. U. S. A.* 114 (2017) 9832.
- [23] X. Yang, Q. j. Li, Z.D. Liu, X. Bai, H.W. Song, M.G. Yao, B. Liu, R. Liu, C. Gong, S.C. Lu, Z. Yao, D.M. Li, J. Liu, Z.Q. Chen, B. Zou, T. Cui, B.B. Liu, *J. Phys. Chem. C* 117 (2013) 8503.
- [24] Y. Wang, S.Q. Jiang, A.F. Goncharov, F.A. Gorelli, X.J. Chen, D. Plášienka, R. Martoňák, E. Tosatti, M. Santoro, *J. Chem. Phys.* 148 (2018), 014503.
- [25] Y.G. Zou, B.B. Liu, L.C. Wang, D.D. Liu, S.D. Yu, P. Wang, T.Y. Wang, M.G. Yao, Q.J. Li, B. Zou, Tian Cui, Guangtian Zou, Thomas Wägberg, Bertil Sundqvist, H.K. Mao, *Proc. Natl. Acad. Sci. U. S. A.* 106 (2009), 22135.
- [26] X.J. Chen, V.V. Struzhkin, Y. Yu, A.F. Goncharov, C.T. Lin, H.K. Mao, R.J. Hemley, *Nature* 466 (2010) 950.
- [27] Z. Zhao, H.J. Zhang, H.T. Yuan, S.B. Wang, Y. Lin, Q.S. Zeng, G. Xu, Z.X. Liu, G.K. Solanki, K.D. Patel, Y. Cui, Harold Y. Hwang, Wendy L. Mao, *Nat. Commun.* 6 (2015) 7312.
- [28] A.P. Drozdov, M.I. Eremets, I.A. Troyan, V. Ksenofontov, S.I. Shylin, *Nature* 525 (2015) 73.
- [29] S.H. Wang, L. Guo, X.G. Wen, S.H. Yang, J. Zhao, J. Liu, Z.H. Wu, *Mater. Chem. Phys.* 75 (2002) 32.
- [30] D. Santamaria-Perez, G. Garbarino, R. Chulia-Jordan, M.A. Dobrowolski, C. Mühle, M. Jansen, *J. Alloys Compd.* 610 (2014) 645.
- [31] A.P. Hammersley, S.O. Svensson, M. Hanfland, A.N. Fitch, D. Häusermann, *High Press. Res.* 14 (1996) 235.
- [32] H.K. Mao, P.M. Bell, J.W. Shaner, D.J. Steinberg, *J. Appl. Phys.* 49 (1978) 3276.
- [33] D. Errandonea, Y. Meng, M. Somayazulu, D. Häusermann, *Physica B* 355 (2005) 116.
- [34] D. Errandonea, A. Muñoz, J. Gonzalez-Platas, *J. Appl. Phys.* (2014), 216101, 115115.
- [35] F. Birch, *J. Appl. Phys.* 9 (1938) 279.
- [36] H. Chi, H. Kim, J.C. Thomas, G.S. Shi, K. Sun, M. Abeykoon, E.S. Bozin, X.Y. Shi, Q. Li, X. Shi, E. Kioupakis, A. Van der Ven, M. Kaviani, C. Uher, *Phys. Rev. B: Condens. Matter Mater.* 89 (2014) 195209.
- [37] J.S. Rhyee, K.H. Lee, S.M. Lee, E. Cho, S.I. Kim, E. Lee, Y.S. Kwon, J.H. Shim, G. Kotliar, *Nature* 459 (2009) 965.
- [38] A.L. Chen, P.Y. Yu, *Phys. Rev. Lett.* 71 (1993) 4011.